Revision 1

Aluminosilicate melts and glasses at 1 to 3 GPa: Temperature and pressure effects on recovered structural and density changes

Saurav Bista[1]*, Jonathan F. Stebbins[1], William B. Hankins[2] and Thomas W. Sisson[2]

[1] Department of Geological and Environmental Sciences, Stanford University, Stanford CA 94305, U.S.A.

[2] Volcano Science Center, U.S. Geological Survey, Menlo Park, CA

*corresponding author, sbista@stanford.edu

Abstract

In the pressure range in the Earth's mantle where many basaltic magmas are generated (1 to 3 GPa) (Stolper et al. 1981), increases in the coordination numbers of the network forming cations in aluminosilicate melts have generally been considered to be minor, although effects on silicon and particularly on aluminum coordination in non-bridging oxygen rich glasses from the higher, 5 to 12 GPa range, are now well known. Most high-precision measurements of network cation coordination in such samples have been made by spectroscopy (notably ^{27}Al and ^{29}Si NMR) on glasses quenched from high temperature, high pressure melts synthesized in solid media apparatuses and decompressed to room temperature and 1 bar pressure. There are several effects which could lead to the underestimation of the extent of actual structural (and density) changes in high pressure/temperature melts from such data. For non-bridging oxygen rich sodium and calcium aluminosilicate compositions in the 1 to 3 GPa range, we show here that glasses annealed near to their glass transition temperatures systematically record higher recovered increases in aluminum coordination and in density than samples quenched from high temperature melts. In the piston-cylinder apparatus used, rates of cooling through the glass transition are measured as very similar for both higher and lower initial temperatures, indicating that fictive temperature effects are not the likely explanation of these differences. Instead, transient decreases in melt pressure during thermal quenching, which may be especially large for high initial run temperatures, of as much as 0.5 to 1 GPa, may be responsible. As a result, the equilibrium proportion of high-coordinated Al in this pressure range may be 50 to 90% greater than previously estimated, reaching mean coordination numbers (e.g. 4.5) that are probably high enough to significantly affect melt properties. New data on jadeite ($NaAlSi_2O_6$) glass confirm that aluminum coordination increase with pressure is inhibited in compositions low in non-bridging oxygens.

Introduction

Structural changes with pressure in silicate melts influence how those melts segregate from their sources and ascend toward Earth's surface, or potentially sink deep into its interior. Quantitative understanding of the response of melt structure to pressure is necessary to predict accurately such properties as density, viscosity and phase equilibria of magmas in the Earth's interior, particularly to extrapolate these properties to conditions difficult or impossible to access experimentally. Much of what we know about such changes comes from diffraction and spectroscopic studies, carried out at room temperature and 1 bar pressure ("ex-situ" conditions) of glasses quenched from melts synthesized at

high temperature and pressure, although in-situ measurements at high temperature and pressure are becoming more accurate (Sakamaki et al. 2012; Wang et al. 2014) and are uniquely important in observing possibly unquenchable structural changes. Much of the recent ex-situ work on high pressure glasses of interest in the Earth sciences, as well as in advanced technologies, has used nuclear magnetic resonance (NMR) to detect increases in the coordination numbers of the network forming cations Si, Al and B, as well as the compression of "soft" cation sites such as Na (Xue et al. 1991; Yarger et al. 1995; Du et al. 2004; Lee et al. 2004; Allwardt et al. 2005a; Kelsey et al. 2009b). Such cation coordination number increases are thought to be fundamental to many melt properties and can now often be accurately quantified; in geologically interesting aluminosilicate glasses, ^{27}Al NMR is especially sensitive to changes in Al cation environments. There has also been considerable complementary work on oxygen speciation studied with ^{17}O NMR (Xue et al. 1994; Lee 2003; Allwardt et al. 2004, 2005; Lee et al. 2006, 2008) as such anionic speciation is the critical complement to that of the network cations. The majority of these studies have used multi-anvil, solid media high pressure apparatuses to produce pressures where recoverable changes in network structure are relatively large but glasses can still be formed, typically 5 to 12 GPa, and in large enough samples (a few to 10's of mg). However, some increases in aluminum coordination (Allwardt et al. 2007; Malfait et al. 2012), as well as more subtle changes in network topology (Mysen and Richet 2005) have been detected in aluminosilicate glasses quenched from melts at 2-3 GPa in piston-cylinder apparatuses. There are also a growing number of studies at 0.1 to 1 GPa with gas pressure apparatuses and run temperatures near to the glass transition temperature (T_g) that explore relaxation kinetics (Wondraczek et al. 2007, 2010; Wu et al. 2009; Smedskjaer et al. 2014). Some of these have also clearly detected significant network structural changes using NMR.

These types of recovered, pressure-induced structural changes can be accurately studied under ex-situ conditions and can be quite useful for deducing general effects of composition (e.g. modifier cation field strength, non-bridging oxygen content, etc.) on expected high pressure changes in melts, in finding correlations between structure and measured property changes (e.g. density), and in establishing mechanisms such as the conversion of non-bridging to bridging oxygen as Si, Al, and B coordination increase. However, these changes as seen in quenched, decompressed glasses have sometimes been considered to represent the lower bounds on the actual effects of pressure on the equilibrium melt at high P and T for several reasons. For example, there is some evidence for relaxation of the network structure during decompression from very high pressures in diamond anvil cells, especially for glasses compressed at ambient temperature but also possibly for samples heated above the glass transition (Farber and Williams 1996; Majérus et al. 2004). In a few multi-anvil apparatus

studies (Allwardt et al. 2005a), faster ambient temperature decompression did seem to retain somewhat greater structural changes in the glasses. More recent work on aluminosilicates to 3.5 GPa, however, indicates that such inelastic density relaxation during glass decompression can be negligible at least in some ranges of composition, suggesting minimal structural changes during return to 1 bar pressure (Malfait et al. 2014). Apart from this issue, the recovered glass structure, corrected for effects of *elastic* compression (to the high pressure, room temperature state of the glass) and of thermal expansion at high pressure (to reach the high P/T liquid), should at best resemble that of the melt at the run pressure and the temperature (T_g) at which the metastable liquid quenches to the glass. There are likely to be additional, possibly important, but as yet poorly known, effects of temperature on the structure on heating above T_g to the solidus-liquidus temperature ranges of most common interest in petrology and geophysics.

Particularly in solid-media high pressure apparatuses, there is in addition the possibility of other poorly-understood effects on the recovered glass of the actual pressure/temperature path followed during quenching of the high temperature melt. For example, in a multi-anvil study at 10 GPa, Allwardt et al. (2005b) noted a large increase in recovered Al coordination number for an albite ($NaAlSi_3O_8$) glass when comparing samples quenched from above the liquidus with those heated near to the glass transition, and a smaller, opposite effect from a non-bridging oxygen rich Na aluminosilicate. This was interpreted in terms of effects of cooling rate, although the possibility of transient melt pressure drops was considered and could not be ruled out. (Faster cooling of a glass-forming liquid quenches in its structure at a higher "fictive temperature" T_f than does slower cooling; for the same cooling rate through the glass transition, initial temperature itself should not affect the quenched-in structure of a single-phase liquid *if* cooling is truly isobaric and isochemical.) In detailed studies of relaxation kinetics at high pressure for albite glass, Gaudio et al. (2009, 2012) reported both temperature effects on density and structure as well as enhanced structural changes from glasses equilibrated near to the glass transition. Gaudio et al. (in press) report details of significant pressure drops during quenching of albite melt from high temperatures in a multianvil apparatus, which lower the recovered density and structural changes relative to those observed in glasses annealed near the glass transition temperature.

Here, we further investigate the effects of thermal history on quenched-in glass structure at high pressures and temperatures using two aluminosilicate glasses known to have large changes in aluminum coordination with pressure and a third glass to represent compositions with very low non-bridging oxygen content (Bista et al. 2013, 2014). The latter is thought to be especially important in

controlling how rapidly network cation coordination increases with pressure in melts and glasses (Allwardt et al. 2004, 2005c; Lee et al. 2004). We explore the range of 1 to 3 GPa, typical of the pressures of basaltic magma genesis in the upper mantle of the modern Earth, focusing on the differences in experimental P/T path and recovered structural changes for initial temperatures above the liquidus vs. near to T_g. We conclude that Al coordination increases preserved in the samples from high temperature are less than equilibrium values at nominal run pressures because of significant decreases in pressure of the sample during quenching; this problem is nearly eliminated by quenching samples from just above T_g. Melt network structure (as sampled by Al coordination number) can change significantly from 1 bar pressure to the upper mantle pressure interval where most basaltic magmas form.

Experimental methods and data analysis

Sodium aluminosilicate ($25.5Na_2O$-$0.5Al_2O_3$-$74SiO_2$, NS3) and calcium aluminosilicate ($30CaO$-$10Al_2O_3$-$60SiO_2$, CAS) glasses (compositions in oxide mole percent) were chosen to study pressure induced structural changes, as both of these compositions are known from previous work at 3 to 10 GPa to show large, recoverable changes in aluminum coordination with pressure (Allwardt et al. 2005a; Allwardt et al. 2007; Kelsey et al. 2009b). Both have relatively high concentrations of non-bridging oxygens (NBO), with nominal NBO per tetrahedral cation of 0.68 (NS3) and 0.75 (CAS) respectively. Jadeite composition glass ($NaAlSi_2O_6$) is also included in this study, because its NBO content should be very low (Thompson and Stebbins 2011), suggesting a different structural response to pressure. Ambient pressure glasses were prepared from reagent grade Al_2O_3, SiO_2, Na_2CO_3 and $CaCO_3$ with 0.1 wt% Co_3O_4 added to speed the spin-lattice relaxation rates. Each mixture was ground together, decarbonated, then melted and ground twice to obtain a homogeneous glass. The compositions of CAS and jadeite glass were checked by electron microprobe analysis and the analyzed compositions are given in Table 1. Both glasses were close to their nominal compositions (within 0.6% for CAS and 2% for jadeite glass). The NS3 composition was taken as nominal because of difficulty in accurate EPMA analysis of alkali-rich silicate glasses.

High pressure samples were made in an end-loaded piston-cylinder apparatus at the USGS, Menlo Park. The 25.4 mm diameter assembly consisted of a calcium fluoride pressure medium (pressed and fired from sized powder), a cylindrical graphite heater, and a 5 mm diameter platinum capsule

sealed by welding. Typical sample masses were 95-115 mg, but samples as large as 150 mg were employed early in the study. Pressure in these assemblies is calibrated by bracketing the melting curve for dried, high-purity CsCl (Clark 1959 as corrected by Bohlen 1984) and by bracketing the quartz-coesite reaction (Bose and Ganguly 1995). Temperature was measured and controlled with type-S thermocouples. Reported temperatures are corrected for the temperature dependent thermal gradient between the measurement position and the sample center (+10 ^{o}C at 1200 ^{o}C, +4 ^{o}C at 750 ^{o}C, negligible <750 ^{o}C) based on prior calibrations with multiple-junction thermocouples.

NS3 samples were held at two different temperatures- above the melting point and near to the glass transition temperature (T_g), the latter as measured at ambient pressure. Samples were held at high pressure and temperature for at least an hour to achieve mechanical and thermal equilibrium of the furnace assembly. Although the goal of this study was not to obtain details of relaxation kinetics or possible effects of pressure on T_g (Gaudio and Lesher 2014), we did conduct experiments on each of the three compositions at varying temperatures near to T_g and for varying run times, to verify complete structural relaxation at pressure.

Samples were quenched at high pressure by switching off power to the furnace; cooling rates were monitored with the thermocouple in the furnace assembly and digitally recorded. During quenching, the measured drop in hydraulic oil pressure, converted to an apparent pressure change of the sample, was approximately -75 MPa to -150 MPa from high temperature to T_g and -150 MPa from T_g to room temperature. Experience with calibrations shows that sample pressure lags hydraulic fluid pressure, so the true pressure drop of the sample would be greater than these values.

Glasses were inspected for crystals with a petrographic microscope and ^{27}Al and/or ^{29}Si MAS NMR. For the compositions studied here, samples quenched from above the liquidus remained glassy. Those quenched from near to T_g, because they were initially heated in the supercooled liquid region, sometimes partially crystallized if the run duration was too long or if the temperature increase above T_g was too large (crystal nucleation and growth rates can increase rapidly with higher T in this range as viscosity drops). In such cases, glassy samples were obtained by lowering run temperature or hold time. Because of temperature limitations of the large diameter furnace assembly, new high temperature (above liquidus) experiments for the CAS composition were done only at 1 GPa. For higher pressures, previously collected NMR spectra for glass samples made in a piston cylinder apparatus at the Department of Geology and Geophysics, Univ. of Minnesota (2 GPa, 1550 ˚C, 3 GPa, 1600 ˚C, Allwardt

2005a; Allwardt et al. 2007) were re-analyzed for comparison with new data from samples quenched from these pressures and temperatures near T_g.

Ambient pressure onset of the T_g was measured in a differential scanning calorimeter (DSC) using a Netzsch 404F3 instrument and was found to be 484 °C, 783 °C and 740 °C for NS3, CAS and jadeite glass respectively. To determine the effect of cooling rate on the fictive temperature (T_f), glasses were initially heated in the DSC, then cooled and reheated at 5, 10, 15, 20 and 25 K/min. The activation energy for relaxation near T_g at ambient pressure for each glass was then calculated (as described in more detail in a previous study, Wu et al. 2011) from the equation:

$$-\frac{\Delta H_a}{2.3R} = \frac{\log q1 - \log q2}{\left[\frac{1}{T_{f1}} - \frac{1}{T_{f2}}\right]} \quad (1)$$

where H_a is the activation energy near T_g, q1 and q2 are two cooling rates and T_{f1} and T_{f2} are the corresponding fictive temperatures. For each glass quenched from high pressure, changes in T_f with variations in measured cooling rates were approximated from the above equation using the calculated activation enthalpy. For comparison purposes, these *differences* in T_f were referenced to the ambient pressure T_g and are reported in Table 3**:** actual T_g values at high pressure were not measured here.

Densities of the glasses were measured with a high precision sink-float technique using diiodomethane-acetone solutions (Kelsey et al. 2009b). The accuracy of the experiment was determined by including silica glass with the well-known density of 2.23 g/cm^3 in our measurements. The absolute uncertainty of our measurements determined from the silica glass is ±0.02 g/cm^3, which is similar to that reported in previous studies (Allwardt 2005a; Allwardt et al. 2007; Kelsey et al. 2009b). The *relative* density changes, however, are much more precise, ±0.001, due to larger samples and repeated measurements.

^{27}Al and ^{23}Na MAS NMR spectra were collected with Varian/Chemagnetics "T3" probes, using Varian 18.8 Tesla (208.4 MHz for ^{27}Al) and 14.1 Tesla (158.7 MHz for ^{23}Na, 156.4 MHz for ^{27}Al) spectrometers. Single pulse acquisitions were used with pulse widths corresponding to approximately 30° radiofrequency tip angles (solid) and recycle delays of 0.1 second for the glasses. Some experiments were done with delays to 10 s as needed to characterize more slowly relaxing crystalline phases. Samples were spun in 3.2 mm zirconia rotors at 20 kHz. The ^{27}Al and ^{23}Na chemical shifts are reported relative to 0.1 M aqueous $Al(NO_3)_3$ and 1 M aqueous NaCl respectively. The ^{27}Al MAS spectra were

background subtracted to remove very small signals from traces of Al in the rotors. The ^{27}Al MAS spectra were analyzed with DMFIT software using the Czjzek distribution of quadrupolar coupling constants (C_Q) (Massiot et al. 2002) to fit the peaks for the differently coordinated aluminum species, and a combination of Gaussian and Lorentzian peak shapes for the spinning sidebands. In our previous studies (Allwardt 2005a; Allwardt et al. 2007) of the CAS composition, ^{27}Al MAS spectra were fitted using multiple Gaussian peaks to account for the non-Gaussian peak shapes. Here, these data have been refitted with DMFIT for consistency and compared with the results of our current study. ^{27}Al 3QMAS spectra were collected using a shifted echo pulse sequence, comprising hard pulse of duration 2.7 μs and 0.8 μs and a soft pulse with duration 17 μs (Massiot et al. 1996) with sample spinning speed of 20 kHz. The ^{27}Al 3QMAS data were processed using the software package, RMN (FAT) (P.J. Grandinetti, The Ohio State University).

Results

Glass densities

The densities for NS3, CAS and jadeite glasses quenched from different pressures and temperatures, relative to those of the 1 bar pressure, as-quenched glasses, are given in Table 2. In Figure 1, relative density versus pressure is plotted for NS3, which shows a clear trend of increasing densification with the increase in pressure. Also, from Figure 1, we observe that the densification increases considerably from the high temperature (1200 °C) to the low temperature (510 °C) sample for a given pressure. The 1 GPa CAS glass also shows densification increases between high temperature (1350 °C) and low temperature (850 °C) experiments. Table 2 also includes densities for CAS glasses from high temperatures and 2 and 3 GPa measured in a previous study (Allwardt et al. 2007). The densification of that 3 GPa glass is substantially less than for the new low temperature sample from this pressure; for the two 2 GPa glasses there is very little difference and it is in the opposite sense, but we suspect that the earlier measurements (Allwardt et al. 2007) are less precise because of smaller sample sizes (a few mg vs. 10's of mg). High pressure jadeite glasses, heated near to T_g, also show densification roughly comparable to the NS3 and CAS glasses.

^{27}Al NMR spectra

Figures 2 and 3 show typical ^{27}Al MAS spectra for NS3 and CAS glasses, quenched from various pressures. As described in a number of previous studies (Allwardt et al. 2005b; Allwardt et al. 2007; Kelsey et al. 2009b), three peaks are resolved, which can be uniquely assigned to four, five, and six-coordinated Al (^{IV}Al, ^{V}Al, ^{VI}Al). At this high magnetic field (18.8 Tesla), peak widths are dominated by chemical shift distributions, but quadrupolar broadening does contribute to peak asymmetry (skewing of peak to the lower frequency, right hand side), especially for the CAS glasses.

Structural relaxation in low temperature runs was confirmed by conducting high pressure experiments at several temperatures near T_g and varying time durations and comparing their spectra. For example, shown in Figure 4B are the spectra of NS3 glasses quenched from 4 hr runs at 470 °C, 490 °C and 510 °C at 2 GPa overlaid for comparison, which shows small differences that don't rely on relative areas calculated from peak fitting. The concentrations of ^{V}Al, ^{VI}Al, which should increase with time as the sample relaxes at P and T until the structure of the metastable supercooled liquid is reached, are similar in all three of the glasses recovered from these experiments. The sample from 490 °C has slightly greater amounts of high coordinated aluminum species; those from 470 °C and 510 ˚C have nearly identical but slightly lower concentrations. These small differences could result from small variations in run pressure, or from somewhat incomplete relaxation at the lowest temperature tested. It is also possible that the slight difference between the 490 and 510 ˚C samples could be a minor effect of fictive temperature, which we have not explored in detail in this study. No differences were observed between samples held at 510 °C, 2 GPa for 1 hour and 8 hours (Fig. 4A) which confirmed that this composition should be fully relaxed in our standard run duration of 4 hours at this temperature. For our CAS glass, experiments were done at 790 °C and 850 °C at 2 GPa for 4 hours (Fig. 5). Only very slight differences exist between these two; the low temperature runs for CAS glasses were therefore done at 850 °C.

Figure 2 shows spectra of NS3 glasses quenched at ambient and high pressures, and for the latter compares data for run temperatures near to T_g (510 ˚C) and above the melting point (1200 ˚C). Spectra for the CAS glasses are shown in Figure 3, which compares data from our 850 ˚C, 2 and 3 GPa runs with spectra collected on glasses from these pressures and 1550 to 1650 ˚C as described in a previous report (Allwardt et al. 2007). Data on Al speciation, derived from consistent fits to all spectra, are given in Table 2. In all cases, there is considerably more high-coordinated Al (both ^{V}Al and ^{VI}Al) in the glasses from the lower temperature runs.

Concentrations of both ^{V}Al and ^{VI}Al increase systematically with pressure for both low temperature and high temperature glasses. For comparison with previous studies, Figures 6 and 7 plot

the average aluminum coordination versus pressure for NS3 and CAS glasses respectively. As in plots of relative density, these plots clearly demonstrate the systematically greater quenched-in structural changes for the lower temperature glasses relative to those from runs above the melting points. For both of these compositions, the figures show relatively small Al coordination increases up to 1 GPa, followed by more significant effects at higher pressures. For comparison with data for glasses quenched from high temperatures melts in multi-anvil apparatus, points for the NS3 composition from 6 GPa (Kelsey et al. 2009b) and for CAS from 5 GPa (Allwardt et al. 2007, standard decompression rate, refitted with DMFIT) are included. Mean C_Q values for the predominant ^{IV}Al sites, estimated from the fits of the 1-D MAS spectra, increase from about 4.0 to about 4.3 MHz with increasing quench pressure for NS3 glass; for CAS glass a slight increase with pressure from about 6.7 to 7.8 MHz was seen. These relative trends are similar to those reported very recently for albite glass quenched from pressures to about 7 GPa (Gaudio et al., in press), and may be due to increasing tetrahedral site distortion, possibly related to higher contents of ^{V}Al and ^{Vi}Al.

For jadeite glass, we conducted high pressure experiments only at temperatures near to T_g. An initial high pressure experiment at 2 GPa was done for 2 hours at 740 °C that resulted in considerable crystallization, suggesting that this was well above T_g at this pressure. A completely glassy sample was then obtained at 2 GPa and 710 ˚C (Fig. 8). Similarly at 3 GPa, a reduced temperature of 670 ˚C was required to obtain a glass with only a very minor amount of crystalline jadeite. A decrease in T_g at higher pressure is implied, consistent with recent detailed work on albite ($NaAlSi_3O_8$) glass relaxation kinetics at 2.6 to 7 GPa (Gaudio and Lesher 2014). The 1-D ^{27}Al MAS NMR spectra (18.8 T) of jadeite glass from various pressures in Figure 8 show a small peak due to ^{V}Al (0.5%) only in the 3 GPa glass. The latter spectrum also indicates the presence of a small amount (<0.01%) of ^{VI}Al in a crystalline phase, probably jadeite (Kelsey et al. 2009b). A triple quantum (3QMAS) spectrum (14.1 T), where broadening from quadrupolar interactions are eliminated (Lee et al. 2004) for the latter sample is given in Figure 9. Here again, a small concentration of ^{V}Al can be seen in the isotropic dimension projection, although its peak is below the lowest contour in the 2-D plot. The 3QMAS spectrum for the 3 GPa CAS glass is included for comparison, and, like the 1-D spectrum, clearly shows large concentrations of ^{V}Al and ^{VI}Al.

^{23}Na NMR

Figure 10 shows the ^{23}Na MAS NMR spectra of NS3 ambient pressure glass and high pressure glass quenched from 510 °C at 2 GPa. The difference in peak position is small (1 to 2 ppm to higher

frequency) but reproducible and in the same direction as the larger shift observed in a previous study (Kelsey et al., 2009b) of a 6 GPa glass of the same composition. The near constancy of peak shape suggests that this change is primarily due to an increase in mean isotropic chemical shift (to higher frequency) for the high pressure sample, which in turn is consistent with a decrease in mean Na-O distance and compression of the Na site. Similar findings have been reported in more extensive previous studies of glasses quenched from high temperature and pressure (Xue and Stebbins 1993; Kelsey et al. 2009a,b), as well as with a recent report on *in situ*, high pressure ^{23}Na NMR on albite glass compressed at room temperature (Gaudio et al. 2015).

Possible effects of fictive temperature

At a given pressure, the point at which the structure of a cooling, metastable liquid is effectively "frozen into" that of a glassy solid is approximated by the fictive temperature, T_f, which is higher at faster cooling rates. Previous studies of ambient pressure aluminosilicate glasses have shown changes in aluminum coordination with fictive temperature (Kiczenski et al. 2005; Stebbins et al. 2008), and work on albite ($NaAlSi_3O_8$) glass at pressures to 7 GPa has also suggested such changes (Gaudio et al. 2009). As shown in Table 3, cooling rates near to T_g are actually quite similar for starting temperatures just above T_g and for those well above the liquidus for both NS3 and CAS compositions, in experiments done at 2 GPa. Given that T_f scales with the logarithm of the cooling rate, this observation means that T_f differences for the glasses with varying initial temperatures are, in this apparatus, very small. Using equation (1), the ambient pressure activation energy for relaxation near T_g (derived from our DSC measurements) and the measured cooling rates, we estimate that the difference in T_f between high temperature and low initial temperatures must be very small in our high pressure experiments (only 2 °C). Given that T_f effects on Al coordination in ambient pressure glasses can usually only be detected by NMR on samples formed with cooling rates varying by several orders of magnitude (Stebbins et al. 2008), it is thus unlikely that the structural changes observed here, or those reported in our previous study of high pressure sodium aluminosilicates (Allwardt et al. 2005b) are in fact dominated by cooling rate differences between high and low temperature experiments. We note that the rates at the onset of cooling from liquidus temperatures are indeed considerably faster (about 79 °C/S for NS3), which may be important for the alternative explanation given below.

Discussion

In our previous study of thermal history effects on structural changes retained in high pressure glasses, we noted a large increase in concentrations of ^{V}Al and ^{VI}Al in albite ($NaAlSi_3O_8$) glass annealed near to T_g, relative to samples quenched from above the liquidus; a much smaller effect in the opposite direction was seen for an NBO-rich sodium aluminosilicate on the albite-sodium tetrasilicate join ($Na_3AlSi_7O_{17}$) (Allwardt et al. 2005b). At that time, effects of cooling rate (fictive temperature) seemed the most likely explanation for these changes, although the possibility of a transient pressure drop during quench from high temperature was also considered. A more recent study of albite glass and melt at pressures to 7 GPa also reported considerably higher Al coordination in glasses annealed near T_g than in those quenched from high temperature liquids (Gaudio et al. 2009, 2012). Other recent data that quantifies some T_f effects on structure (Stebbins et al. 2008), and our measurements presented here of high pressure cooling rates and effects of initial temperature, all indicate that the latter hypothesis (pressure drop during quench from high T) is indeed likely to be the most important explanation, as documented further in a very recent study of albite glass (Gaudio et al., in press). Our previous result of an apparent effect in the opposite direction for the $Na_3AlSi_7O_{17}$ glass seems anomalous in this context, but could possibly be explained by a lack of complete structural relaxation at high pressure in that experiment: T_g was not measured for that sample and experiments to test the extent of relaxation were not done.

Our structural and density data on high vs. low temperature NS3 glasses (Table 2 and Fig. 1 and 6) suggest that the decrease of pressure on the melt during quench from 2 GPa in the 2.54 cm piston cylinder apparatus is about 0.5 GPa: for example, the Al coordination of the glass quenched from 510 °C at 1.5 GPa and 1200 °C and 2 GPa are similar. Comparison of new data on low temperature runs on CAS glasses with our previous samples from high temperatures and 2 to 3 GPa (Fig. 3) suggests that melt pressure drops could be even larger (as much as 1 GPa for an initial P of 3 GPa), although this comparison is less direct because those high temperature samples were made in a different laboratory and such effects are likely to depend somewhat on details of the equipment and assemblies used. As is typical for most solid-media high pressure apparatus, we observed reductions in hydraulic oil pressure during quench, but measured values correspond to considerably smaller sample pressure drops, of only about 0.075 to 0.15 GPa from 1200 °C to 510 °C. Such relatively minor pressure drops have also been reported in recent studies by others of glasses formed by quenching melts in a piston cylinder apparatus (Malfait et al. 2012).

The implication of our new results is thus that melt samples in solid media high pressure apparatus may experience large transient drops in pressure on rapid cooling from super-liquidus temperatures to the glass transition region, which is typically at least 600 to 700 ˚C and may be much greater at higher pressure, e.g. ca. 1700 ˚C in earlier 10 GPa studies mentioned above (Allwardt et al. 2005b). Depending on the sample and heater size, and the type of apparatus and pressure medium, this cooling may occur in a few seconds or less than a second, apparently too short a time for the solid-media system to respond to pressure transients in the liquid sample itself.

A starting point for understanding such transient pressure changes is the "thermal pressure", defined as the isovolumetric change in pressure with temperature and simply related to the thermal expansivity α and the bulk modulus K_T of the melt (Poirier 2000), with $(dP/dT)_V = \alpha K_T$. Both thermodynamic parameters may be functions of T and P; data on the latter are especially limited for simple binary and ternary composition liquids. However, as a rough approximation we can estimate both from compositional fits to ambient pressure melt volumes and compressibilities (Lange and Carmichael 1990), and apply an estimate of the pressure derivative of K_T of 4 (Jing and Karato 2008). At 2 GPa and a temperature drop during quench of 700 ˚C, we estimate the isovolumetric pressure drop for both sample compositions as roughly 0.8 GPa. The calculated decrease in sample pressure is inexact for a real apparatus, where the metal capsule containing the sample and the surrounding pressure medium also respond to quenching, and the metal sample capsule may deform due to resulting pressure differences. The rate of isovolumetric pressure drop for the CaF_2 pressure medium has a rough value of 1.7 MPa/^{o}C derived from room temperature α and K_T. Other widely used solid pressure media have similar to somewhat larger responses of isovolumetric pressure to temperature, NaCl: ~1.1 MPa/^{o}C, $BaCO_3$: ~4.7 MPa/^{o}C. An exception is h-BN: 0.2-0.04 MPa/^{o}C, and use of h-BN pressure assemblies might mitigate some of the decrease in sample pressure during quench. Notably, the pressure drop of the sample could be larger with greater temperature drops during quench, such as those often chosen to ensure melting at much higher pressures as in typical experiments in multi-anvil apparatus (Yarger et al. 1995; Lee et al. 2004; Allwardt et al. 2007; Kelsey et al. 2009a,b). Higher K_T values for melts at higher pressures could also be expected to increase such effects. A further complication arises if T_g is strongly dependent on pressure (Gaudio and Lesher 2014), as the temperature at which the melt structure is quenched into that of the glass will then vary with the magnitude of the pressure drop.

In any case, as long suggested from a variety of considerations (Allwardt et al. 2005b), the structural changes recorded in glasses quenched from melts at high pressure are probably lower limits

393 on those that are actually present in the melts at the nominal run pressure and the high pressure T_g.
394 Experiments conducted near to T_g should avoid large effects of pressure drops as observed here, but can
395 be complicated by uncertain effects of pressure itself on T_g and thus on required run temperatures and
396 durations on structural relaxation, as detailed in recent extensive studies of albite glasses. In many
397 compositions, crystallization of supercooled liquids can be hard to avoid at temperatures above T_g but
398 well below the solidus. Furthermore, structural changes that are present at high pressure and the high
399 temperatures of most interest to petrologists and geophysicists depend as well on still poorly known
400 effects of temperature on structure at high pressures; clearly, in situ structural measurements remain of
401 major importance as indicated by recent progress in this field (Sakamaki et al. 2012).

402 In an important recent study of several aluminosilicates, Malfait et al. (2014) showed that the
403 density of the melts, as measured *in situ* at pressures to 3.5 GPa, can be accurately calculated (within
404 estimated uncertainties) from 1 bar measurements on recovered glass densities and elastic properties.
405 However, small systematic differences between the data sets may be consistent with pressure drop
406 effects comparable to those seen here.

407 Most previous studies of pressure effects on oxide melts and glasses have either been done at
408 ambient temperature, in which case the structure may not relax to its metastable equilibrium state, or
409 on glasses quenched from temperatures high enough to ensure complete melting and thus avoiding
410 crystallization. Both types of experiment can be quite useful, as they can produce glasses whose
411 increased recovered densities (or other physical property changes) can be correlated with recovered,
412 quenched-in structural changes, which can in turn provide insights into mechanisms of structural
413 change, relative effects of composition, etc. For example, a plot of mean Al coordination vs.
414 densification (V/V_0) for CAS and NS3 glasses in Figure 11 shows a significantly steeper slope for the
415 latter, which corresponds well to that seen in previous reports on glasses quenched from higher
416 pressure, high temperature melts (Allwardt et al. 2005a; Kelsey et al. 2009b). Details of the correlation
417 at the lower V/V_0 values seem to be somewhat different, however, perhaps because of different
418 relaxation kinetics for the bulk density and the higher energy processes involved in reconfiguring the
419 glass network structure. The latter has been observed in a recent study of relaxation of densified
420 borosilicate glasses, for example (Smedskjaer et al. 2014), and is expected in systems where the bulk
421 density changes are dominated by compression of "soft" cation environments (e.g. Na^+) and
422 accompanying bond angle changes, and not by coordination changes in the network cations themselves.
423 We have shown that this situation prevails in the types of compositions and pressures studied here

(Allwardt et al. 2005a; Kelsey et al. 2009b; Wu et al. 2009), where measured recovered density increases are much larger than can be simply explained by observed increases in Al coordination.

Implications

In the 2 to 3 GPa range, increases in aluminum coordination in NS3 and CAS melts quenched from near T_g are at least 50 to 90 % higher than values expected from previous experiments on quenched higher temperature melts. In terms of structurally critical compositional variables such as NBO/T, Al/Si, and modifier cation field strength, the latter is a relatively good analog for typical basalt compositions (Allwardt et al. 2005a). It is thus possible that in the regions of the upper mantle where most magma production occurs in the modern Earth, network structural changes may be more significant than considered in current models of properties vs. composition (Lange and Carmichael 1990), component activities and phase equilibria (Ghiorso et al. 2002); in particular as much as 25-35% of the Al may be in coordinations higher than 4. For mafic magmas with high contents of high field strength network modifier cations (Mg^{2+} and Fe^{2+} vs. Ca^{2+}), aluminum coordination changes with pressure should be even more pronounced (Allwardt et al. 2005a). Improved versions of such models may need to consider such changes, as has been long recognized for melt systems at much higher pressures (Ghiorso 2004). An important uncertainty remains in the effects of temperature on Al coordination and other structural changes between T_g and magmatic temperatures. Limited data suggest that Al coordination increases with T in aluminosilicate melts at ambient pressure, but can decrease with T in other systems, e.g. those rich in boron (Stebbins et al. 2008; Morin et al. 2014). Temperature effects *at high pressures* remain uncertain and are a critical area for future research.

Studies of glasses quenched from high temperature melts at high pressure have long suggested that high coordinated Al and Si develop at lower pressures in compositions with abundant NBO (Xue et al. 1991; Yarger et al. 1995; Allwardt et al. 2004; Lee et al. 2004), indicating the possibility of different mechanisms of network structural change in compositions initially low in NBO. The relatively high concentrations of ^{V}Al and ^{VI}Al in albite glasses annealed near to T_g at 10 GPa (Allwardt et al. 2005b) and up to 7 GPa (Gaudio et al. 2009; Gaudio et al., in press) (much higher than those from high T melts) thus raise the question of the true extent of this compositional distinction. Jadeite glass should be nominally free of NBO at ambient pressure, although recent ^{17}O NMR studies of Ca and K aluminosilicates suggest that a few percent of this species might actually be present (Thompson and Stebbins 2011). Our data on this glass annealed near to T_g at 2 and 3 GPa show that indeed, the concentration of ^{V}Al is much less than in the NBO-rich NS3 and CAS compositions, confirming the overall general view of a major

455 difference in high pressure effects with this important compositional/structural variable. In some low-
456 NBO compositions, such as a rhyolite analog, up to about 2 % of this species may be detectable by high-
457 field ^{27}Al MAS NMR in glasses from pressures as low as 2-3 GPa (Malfait et al. 2012), and it is certain to
458 become more abundant at higher pressures. In "depolymerized" mafic and ultramafic melts most
459 abundant in the Earth's upper mantle, however, network speciation changes with pressure are likely to
460 be more dramatic.

461

462 **Acknowledgements**

463 We thank Jodi Puglisi and Corey Liu for access to the 18.8 Tesla spectrometer in the Stanford
464 Magnetic Resonance Laboratory, and Namjun Kim for assistance with collecting these spectra. We also
465 thank Bob Jones for help with the EPMA. We thank Wim Malfait (EMPA, Zürich), Celeste Mercer
466 (U.S.G.S. Denver) and an anonymous reviewer for helpful comments on the manuscript, and Sabyasachi
467 Sen and Sarah Gaudio (U.C. Davis) for many interesting and fruitful discussions about glass structure and
468 relaxation. This work was supported by the NSF, grant EAR-1019596. The experimental facility is
469 supported by the Volcano Hazards Program of the USGS.

470

References Cited:

Allwardt, J.R., Schmidt, B.C., and Stebbins, J.F. (2004) Structural mechanisms of compression and decompression in high-pressure $K_2Si_4O_9$ glasses: an investigation utilizing Raman and NMR spectroscopy of glasses and crystalline materials. Chemical Geology, 213, 137–151.

Allwardt, J.R., Stebbins, J. F., Schmidt, B. C., Frost, D. J., Withers, A. C., and Hirschmann, M.M. (2005a) Aluminum coordination and the densification of high-pressure aluminosilicate glasses. American Mineralogist, 90, 1218–1222.

Allwardt, J.R., Poe, B.T. and Stebbins, J.F. (2005b) The effect of fictive temperature on Al coordination in high-pressure (10 GPa) sodium aluminosilicate glasses. American Mineralogist, 90, 1453–1457.

Allwardt, J.R., Stebbins, J.F., Schmidt, B.C., and Frost, D.J. (2005c) The effect of composition, compression, and decompression on the structure of high-pressure aluminosilicate glasses. An investigation utilizing ^{17}O and ^{27}Al NMR. In Advances in High-Pressure Techniques for Geophysical Applications pp. 211–240. Elsevier.

Allwardt, J.R., Stebbins, J.F., Terasaki, H., Du, L.-S., Frost, D.J., Withers, a. C., Hirschmann, M.M., Suzuki, a., and Ohtani, E. (2007) Effect of structural transitions on properties of high-pressure silicate melts: ^{27}Al NMR, glass densities, and melt viscosities. American Mineralogist, 92, 1093–1104.

Bista, S., Stebbins, J., Hankins, B., and Sisson, T. (2013) Aluminosilicate melts and glasses at 1 to 3 GPa: temperature and pressure effects on recovered structural and density changes. American Geophysical Union Fall Meeting, abstract MR33A-2301

——— (2014) Aluminosilicate Melts and Glasses at 1 to 3 GPa: Temperature and pressure effects on recovered structural and density changes. Goldschmidt Conference, abstracts, 125

Du, L.S., Allwardt, J.R., Schmidt, B.C., and Stebbins, J.F. (2004) Pressure-induced structural changes in a borosilicate glass-forming liquid: Boron coordination, non-bridging oxygens, and network ordering. Journal of Non-Crystalline Solids, 337, 196–200.

Bohlen, S.R. (1984) Equilibria for precise pressure calibration and a frictionless furnace assembly for the piston-cylinder apparatus. Neues Jahrbuch für Geologie, 9, 404-412.

Bose, K., and Ganguly, J. (1995) Quartz-coesite transition revisited: Reversed experimental determination at 500-1200 °C and retrieved thermochemical properties. American Mineralogist, 80, 231-238.

Clark, S.P. (1959) Effect of pressure on the melting points of eight alkali halides. Journal of Chemical Physics, 31, 1526-1531.

Du, L.S., Allwardt, J.R., Schmidt, B.C., and Stebbins, J.F. (2004) Pressure- induced structural changes in a borosilicate glass-forming liquid: Boron coordination, non-bridging oxygens, and network ordering. Journal of Non-Crystalline Solids, 337, 196-200.

Farber, D.L., and Williams, Q. (1996) An in situ Raman spectroscopic study of $Na_2Si_2O_5$ at high pressures and temperatures: Structures of compressed liquids and glasses. American Mineralogist, 81, 273–283.

Gaudio, S., and Lesher, C. (2014) Viscosity of albite melt at high pressure. Goldschmidt Conference, abstracts, 776.

Gaudio, S., Lesher, C., and Sen, S. (2009) Structural and density relaxation in $NaAlSi_3O_8$ glass at high pressure and temperature. American Geophysical Union Fall Meeting, abstract MR433a-1865.

——— (2012) Relaxation in $NaAlSi_3O_8$ across the glass transition interval at high pressure. Glass & Optical Materials Division annual Meeting, GOMD-SI-075-2012.

Gaudio, S.J., Edwards, T.G. and Sen, S. (2015) An in situ high-pressure NMR study of sodium coordination environment compressibility in albite glass. American Mineralogist, 100, 326-329.

Gaudio, S.J., Lesher, C.E., Maekawa, H., Sen, S. (2015) Linking high-pressure structure and density of albite liquid near to the glass transition. Geochimica Cosmochimica Acta (in press).

Ghiorso, M.S. (2004) An equation of state for silicate melts . Model to 40 GPa, 304, 811–838.

Ghiorso, M.S., Hirschmann, M.M., Reiners, P.W., and Kress, V.C. (2002) The pMELTS: A revision of MELTS for improved calculation of phase relations and major element partitioning related to partial melting of the mantle to 3 GPa. Geochemistry, Geophysics, Geosystems, 3, 1–35.

Jing, Z., and Karato, S. (2008) Compositional effect on the pressure derivatives of bulk modulus of silicate melts. Earth and Planetary Science Letters, 272, 429–436.

Kelsey, K.E., Stebbins, J.F., Singer, D.M., Brown, G.E., Mosenfelder, J.L., and Asimow, P.D. (2009a) Cation field strength effects on high pressure aluminosilicate glass structure: Multinuclear NMR and La XAFS results. Geochimica et Cosmochimica Acta, 73, 3914–3933.

Kelsey, K.E., Stebbins, J.F., Mosenfelder, J.L., and Asimow, P.D. (2009b) Simultaneous aluminum, silicon, and sodium coordination changes in 6 GPa sodium aluminosilicate glasses. American Mineralogist, 94, 1205–1215.

Kiczenski, T.J., Du, L.-S., and Stebbins, J. (2005) The effect of fictive temperature on the structure of E-glass: A high resolution, multinuclear NMR study. Journal of Non-Crystalline Solids, 351, 3571–3578.

Lange, R.L., and Carmichael, I.S.E. (1990) Thermodynamic properties of silicate liquids with emphasis on density, thermal expansion and compressibility. Reviews in Mineralogy and Geochemistry, 24, 25–64.

Lee, S., Cody, G., Fei, Y., and Mysen, B. (2006) The effect of Na/Si on the structure of sodium silicate and aluminosilicate glasses quenched from melts at high pressure: A multi-nuclear (Al-27, Na-23, O-17) 1D and 2D solid-state NMR study. Chemical Geology, 229, 162–172.

Lee, S.K. (2003) Order and disorder in sodium silicate glasses and melts at 10 GPa. Geophysical Research Letters, 30, 1845.

Lee, S.K., Cody, G.D., Fei, Y., and Mysen, B.O. (2004) Nature of polymerization and properties of silicate melts and glasses at high pressure. Geochimica et Cosmochimica Acta, 68, 4189–4200.

Lee, S.K., Cody, G.D., Fei, Y., and Mysen, B.O. (2008) Oxygen-17 nuclear magnetic resonance study of the structure of mixed cation calcium-sodium silicate glasses at high pressure: implications for molecular link to element partitioning between silicate liquids and crystals. Journal of Physical Chemistry. B, 112, 11756–61.

Majérus, O., Cormier, L., Itié, J.P., Galoisy, L., Neuville, D.R., and Calas, G. (2004) Pressure-induced Ge coordination change and polyamorphism in SiO_2-GeO_2 glasses. Journal of Non-Crystalline Solids 345–346, 34–38.

Malfait, W.J., Verel, R., Ardia, P., and Sanchez-Valle, C. (2012) Aluminum coordination in rhyolite and andesite glasses and melts: Effect of temperature, pressure, composition and water content. Geochimica et Cosmochimica Acta, 77, 11–26.

Malfait, W.J., Seifert, R., and Sanchez-Valle, C. (2014) Densified glasses as structural proxies for high-pressure melts: configurational compressibility of silicate melts retained in quenched and decompressed glasses. American Mineralogist, 99, 2142-2145.

Massiot, D., Touzo, B., Trumeau, D., Coutures, J.P., Virlet, J., Florian, P., and Grandinetti, P.J. (1996) Two-dimensional magic-angle spinning isotropic reconstruction sequences for quadrupolar nuclei. Solid State Nuclear Magnetic Resonance, 6, 73–83.

Massiot, D., Fayon, F., Capron, M., King, I., Le Calvé, S., Alonso, B., Durand, J.-O., Bujoli, B., Gan, Z., and Hoatson, G. (2002) Modelling one- and two-dimensional solid-state NMR spectra. Magnetic Resonance in Chemistry, 40, 70–76.

Morin, E.I., Wu, J., and Stebbins, J.F. (2014) Modifier cation (Ba, Ca, La, Y) field strength effects on aluminum and boron coordination in aluminoborosilicate glasses: the role of fictive temperature and boron content. Applied Physics A, 116, 479-490.

Mysen, B.O., and Richet, P., Eds. (2005) Aluminosilicate systems: II. Structure. In Silicate Glasses and Melts- Properties and Structure pp. 259–290. Elsevier, Amsterdam.

Poirier, J.-P. (2000) Introduction to the Physics of the Earth's Interior, 2nd ed. pp. 25–26. Cambridge University Press, Cambridge, UK.

Sakamaki, T., Wang, Y., Park, C., Yu, T., and Shen, G. (2012) Structure of jadeite melt at high pressures up to 4.9 GPa. Journal of Applied Physics, 111, 112623.

572 Smedskjaer, M.M., Youngman, R.E., Striepe, S., Potuzak, M., Bauer, U., Deubener, J., Behrens, H., Mauro,
573 J.C., and Yue, Y. (2014) Irreversibility of pressure induced boron speciation change in glass.
574 Scientific Reports, 4, 3770.

575 Stebbins, J.F., Dubinsky, E. V., Kanehashi, K., and Kelsey, K.E. (2008) Temperature effects on non-bridging
576 oxygen and aluminum coordination number in calcium aluminosilicate glasses and melts.
577 Geochimica et Cosmochimica Acta, 72, 910–925.

578 Stolper, E., Walker, D., Hager, B.H., and Hays, J.F. (1981) Melt segregation from partially molten source
579 regions: the Importance of melt density and source region size. Journal of Geophysical Research,
580 86, 6261–6271.

581 Thompson, L.M., and Stebbins, J.F. (2011) Non-bridging oxygen and high-coordinated aluminum in
582 metaluminous and peraluminous calcium and potassium aluminosilicate glasses: High-resolution
583 ^{17}O and ^{27}Al MAS NMR results. American Mineralogist, 96, 841–853.

584 Wang, Y., Sakamaki, T., Skinner, L.B., Jing, Z., Yu, T., Kono, Y., Park, C., Shen, G., Rivers, M.L., and Sutton,
585 S.R. (2014) Atomistic insight into viscosity and density of silicate melts under pressure. Nature
586 Communications, 5, 3241.

587 Wondraczek, L., Behrens, H., Yue, Y., Deubener, J., and Scherer, G.W. (2007) Relaxation and glass
588 transition in an isostatically compressed diopside glass. Journal of the American Ceramic Society,
589 90, 1556–1561.

590 Wondraczek, L., Krolikowski, S., and Behrens, H. (2010) Kinetics of pressure relaxation in a compressed
591 alkali borosilicate glass. Journal of Non-Crystalline Solids, 356, 1859–1862.

592 Wu, J., Deubener, J., Stebbins, J.F., Grygarova, L., Behrens, H., Wondraczek, L., and Yue, Y. (2009)
593 Structural response of a highly viscous aluminoborosilicate melt to isotropic and anisotropic
594 compressions. The Journal of Chemical Physics, 131, 104504.

595 Wu, J., Potuzak, M., and Stebbins, J.F. (2011) High-temperature in situ ^{11}B NMR study of network
596 dynamics in boron-containing glass-forming liquids. Journal of Non-Crystalline Solids, 357, 3944–
597 3951.

598 Xue, X., Stebbins, J.F., and Kanzaki, M. (1994) Correlations between ^{17}O NMR parameters and local
599 structure around oxygen in high-pressure silicates: implications for the structure of silicate melts at
600 high pressure. American Mineralogist, 79, 31–42.

601 Xue, X., and Stebbins, J.F. (1993) ^{23}Na NMR chemical shifts and local Na coordination environments in
602 silicate crystals, melts and glasses. Physics and Chemistry of Minerals, 20, 297–307.

603 Xue, X., Stebbins, J.F., Kanzaki, M., McMillan, P.F., and Poe, B. (1991) Pressure-induced silicon
604 coordination and tetrahedral structural-changes in alkali oxide-silica melts up to 12 GPa - NMR,
605 Raman, and Infrared-Spectroscopy. American Mineralogist, 76, 8–26.

606 Yarger, J.L., Smith, K.H., Nieman, R.A., Diefenbacher, J., Wolf, G.H., Poe, B.T., and McMillan, P.F. (1995)
607 Al coordination changes in high-pressure aluminosilicate liquids. Science, 270, 1964-1967

608

609

610

611

612

613

614 **Table 1.** Compositional analyses from electron microprobe, in mol%

Sample	Na_2O ±0.5	CaO ±0.2	Al_2O_3 ±0.2	SiO_2 ±0.3
CAS		59.1	9.9	31
jadeite	14.6		16.9	68.4

615

616

617 **Table 2.** Experimental conditions, Al- speciation, and relative densities of high pressure glasses

Sample	P (GPa)	T (°C)	^{IV}Al (%) ±0.2	^{V}Al (%) ±0.2	^{VI}Al (%) ±0.2	avg. ^{N}Al ±0.2	relative density*
NS3	1 bar	1200	97.4	2.6		4.02	
NS3	1	1200	95.4	4.7		4.05	1.015(1)
NS3	1	510	90.6	8.7	0.7	4.06	1.021 (1)
NS3	1.5	510	80.4	14.9	4.7	4.24	1.038(1)
NS3	2	1200	81.7	14.4	4.0	4.22	1.032(1)
NS3	2	510	64.3	22.8	12.9	4.48	1.054(1)
CAS	1 bar	1455	96.9	3.1		4.03	
CAS	1	1350	93.9	5.7	0.4	4.07	1.013(1)
CAS	1	850	92.9	6.7	0.35	4.07	1.022(1)
CAS	2	850	78.8	18.7	2.6	4.24	1.052(1)
CAS**	2	1550	86.9	11.8	1.3	4.14	1.059
CAS	3	850	63.7	29.3	7.0	4.43	1.082(1)
CAS**	3	1650	82.3	15.3	2.4	4.20	1.067
jadeite	2	710		<0.3			1.0436(1)
jadeite	3	670	99.5	0.5			1.0672(2)

618

619 *density relative to glass quenched at 1 bar pressure

620 **spectra from previous study (Allwardt et al. 2007) refitted here with DMFIT

621

Table 3. Cooling rates, activation energies for relaxation near T_g and fictive temperatures calculated for NS3 and CAS glasses quenched from different temperatures and 2 GPa.

Sample	Initial temperature (°C)	Cooling rate (°C/s) ±5	Activation enthalpy, ΔH_a (kJ/mol)	Fictive temperature (°C)*
NS3	1200	39	440(90)	501
NS3	510	48	440(90)	503
CAS	1350	72	1013(114)	801
CAS	850	63	1013(114)	800

* calculated assuming ambient pressure T_g, see text.

Figures Captions:

Figure 1. Plot of relative density versus pressure for NS3 glasses quenched from 510 °C and 1200 °C. The 6 GPa datum (triangle) is from previous study (Kelsey et al. 2009b)

Figure 2. ^{27}Al MAS NMR spectra (18.8 T) of NS3 glass from ambient pressure, from 1 GPa - 510 °C (dotted), 1200 °C (solid); and from 2 GPa - 510 °C (dotted), 1200 °C (solid). The asterisk in the 1 GPa, 510 °C spectrum denotes a peak at 4 ppm from a tiny amount of a crystalline phase (< 0.01% of the total peak area).

Figure 3. ^{27}Al MAS NMR spectra (18.8 T) of CAS glass from ambient pressure; from 2 GPa - 850 °C (dotted), 1550 °C (solid); and from 3 GPa - 850 °C (dotted), 1650 °C (solid). Spectra for the two high temperature samples are from previous work (Allwardt et al. 2007)**.**

Figure 4.

A. ^{27}Al MAS NMR spectra (14.1 T) of NS3 glass quenched from 2 GPa and 510 °C following 1 hour (dashed) and 8 hours (solid) run times.
B. ^{27}Al MAS NMR spectra (14.1 T) of NS3 glasses quenched from 470 °C (dotted), 490 °C (thick solid) and 510 °C (dashed) at 2 GPa. The 470 °C data closely overlaps with those of 510 °C.

Figure 5. ^{27}Al MAS NMR spectra of CAS glass (14.1 T) quenched from 850 °C (solid) and 790 °C (dashed) at 2 GPa.

Figure 6. Plot of average aluminum coordination versus pressure for NS3 glasses quenched from 510 °C and 1200 °C. The 6 GPa datum (triangle) is from previous study (Kelsey et al. 2009b)

Figure 7. Plot of average aluminum coordination versus pressure for CAS glasses quenched from low temperature and high temperatures. The high temperature data from 2, 3 and 5 GPa are from previous study (Allwardt et al. 2005a; Allwardt et al. 2007) refitted with DMFIT for consistent comparisons.

Figure 8. ^{27}Al MAS NMR spectra (18.8 T) of jadeite glass quenched from melt at ambient pressure (solid line), quenched from 710 °C at 2 GPa (thick dashed line) and quenched from 670 °C at 3 GPa (thin dotted line). Asterisk marks peak from a tiny amount of a crystalline phase, probably jadeite.

Figure 9. ^{27}Al 3QMAS NMR spectra (14.1 T) for CAS and jadeite glass quenched from near to T_g at varying pressure as labeled. The contour lines are drawn from 5 to 95% for CAS and 2 to 95% for jadeite glass. On the right side, isotropic dimension projections are shown.

Figure 10. ^{23}Na NMR spectra (14.1 T) of NS3 ambient pressure glass (solid) and NS3 glass quenched from 510 °C at 2 GPa (dashed).

Figure 11. Average Al coordination versus densification (expressed as molar volume of high pressure glass divided by that at ambient pressure) for NS3 and CAS glasses. The dashed line segments (CAS* and NS3*) show the average slopes (positions are arbitrary) from previous work on glasses quenched from high temperature melts (Allwardt et al. 2005a; Kelsey et al. 2009b), to illustrate apparent systematic differences in behavior between the two compositions.

682

Figure 1.

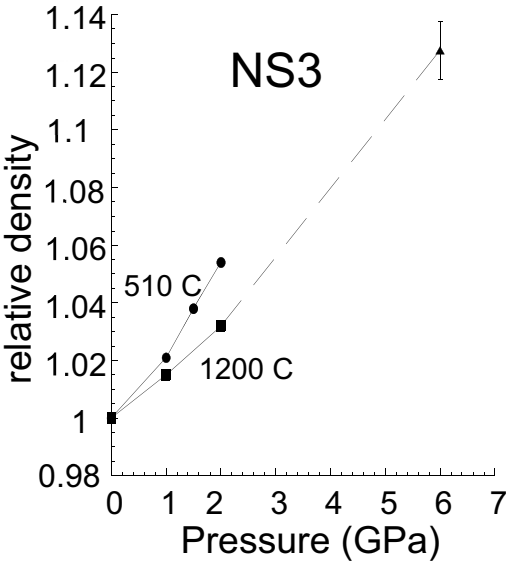

Figure 2.

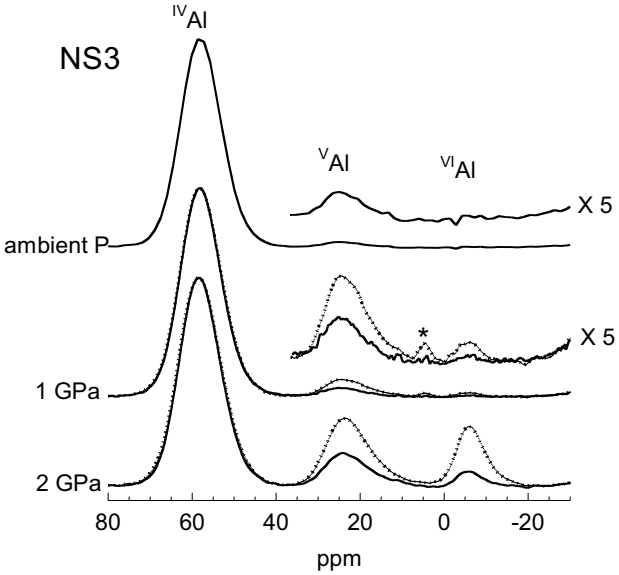

Figure 3.

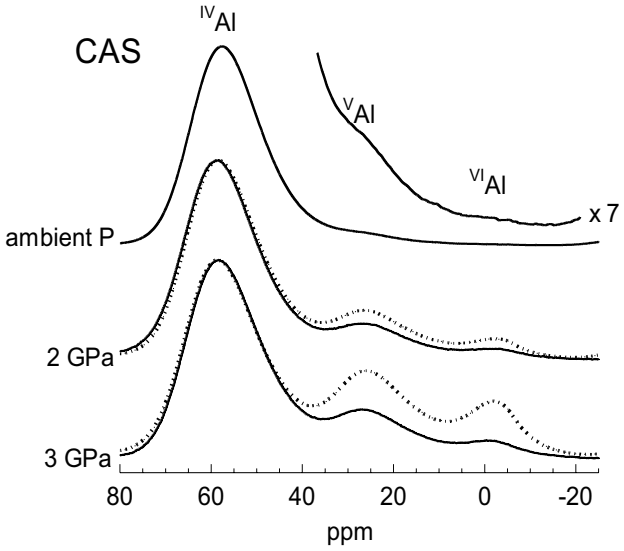

Figure 4.

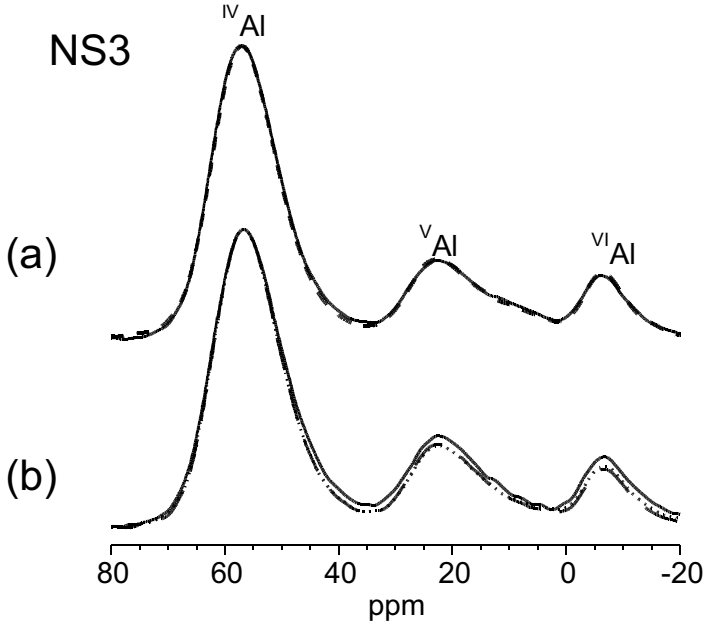

Figure 5.

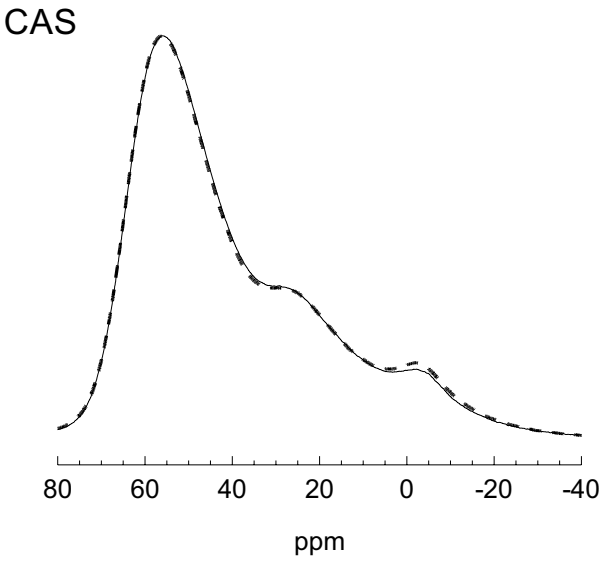

Figure 6.

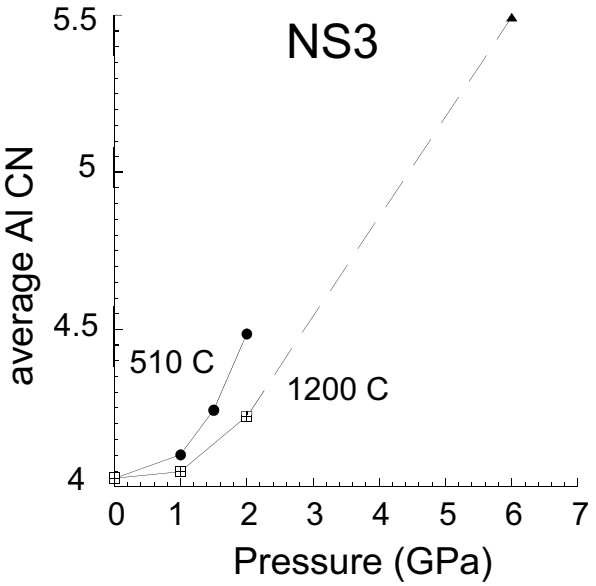

Figure 7.

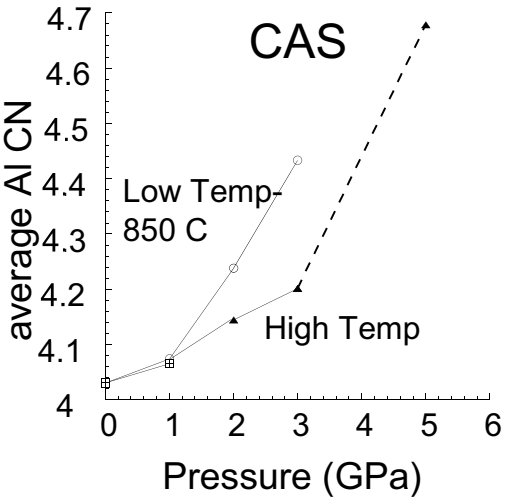

Figure 8.

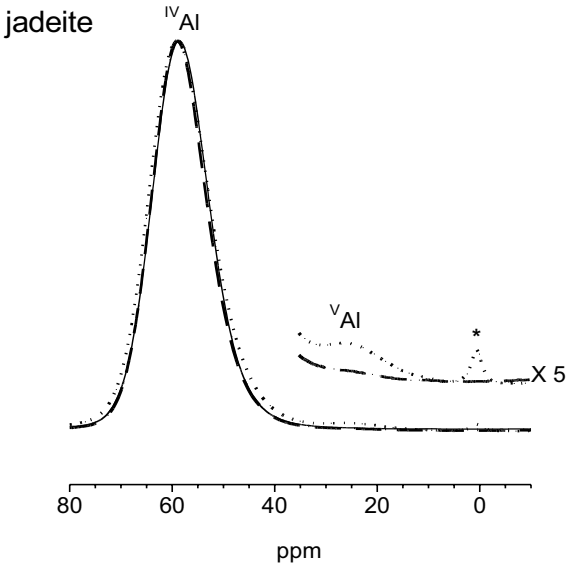

Figure 9.

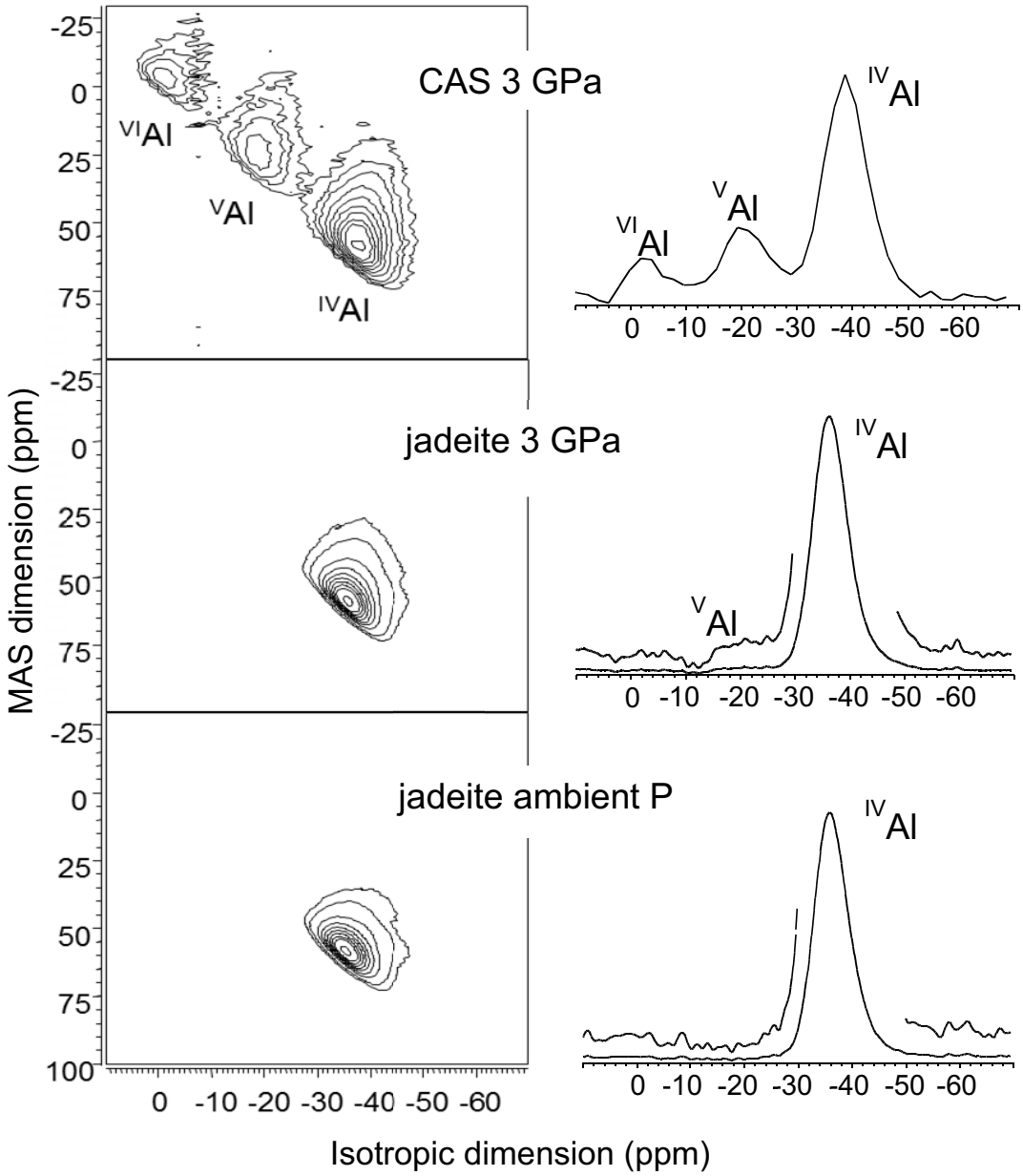

Figure 10.

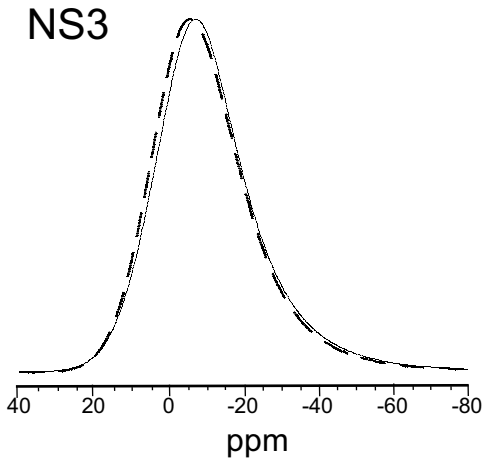

Figure 11.